Denitrification and Anammox and Feammox in the Yinchuan Yellow River wetland

Qingsong Guan^{1,2,3}*, Yiqiao Zhou^{2,3}, Shuo Li^{2,3}, Fan Yang^{2,3}, Rentao Liu¹*

¹Breeding Base for State Key Laboratory of Land Degradation and Ecological Restoration in Northwestern China; Key Laboratory of Restoration and Reconstruction of Degraded Ecosystems in Northwestern China of Ministry of Education, Ningxia University, Yinchuan, P.R. China

Citation: Guan Q.S., Zhou Y.Q., Li S., Yang F., Liu R.T. (2024): Denitrification and Anammox and Feammox in the Yinchuan Yellow River wetland. Plant Soil Environ., 70: 731–738.

Abstract: Denitrification, anaerobic ammonium oxidation (Anammox), and ferric iron reduction coupled with anaerobic ammonium oxidation (Feammox) are the nitrogen removal pathways in natural ecosystems. In this study, the differences between these three nitrogen removal pathways in a *Phragmites australis* covered site (LW), artificial grassland covered site (CD), poplar covered site (YD), and topsoil tillage after harvesting reed site (GD) in the Yinchuan Yellow River wetland were investigated using isotope tracing, metagenome, and quantitative polymerase chain reaction (Q-PCR) techniques. No 30 N $_2$ accumulation was detected in 15 NH $_4^+$ addition incubations, indicating that Feammox was weak in all sites, which is consistent with a low abundance of the Feammox functional bacteria *Acidimiprobiaceae* sp. A6. The denitrification rates were 0.36 (LW), 0.5 (CD), 0.76 (YD) and 0.12 (GD) mg N/kg/day. The Anammox rates were 0.18 (LW) and 0.26 (GD) mg N/kg/day; other sites did not detect Anammox rate. Denitrification was the dominant pathway except for the CD site. The YD site had the highest abundance of denitrification genes, which was consistent with the denitrification rate.

Keywords: nitrogen cycling; environmental microorganism; functional gene; iron-nitrogen coupling; biogeochemistry

Nitrogen cycling is one of the most important processes in natural ecosystems (Gruber and Galloway 2008), and nitrogen removal is an important process for maintaining the health of natural ecosystems. It is also an important topic in nitrogen cycling research (Fowler et al. 2013). The denitrification process $(NO_3^- \to NO_2^- \to NO \to N_2O \to N_2)$ was once considered to be the only pathway by which nitrogen from

the soil could return to the atmosphere, completing the ecological loop of nitrogen turnover from the soil to the atmosphere (Delwiche and Bryan 1976, Niu et al. 2021). In recent years, the discovery of anaerobic ammonia oxidation (Anammox $\mathrm{NH_4^+} + \mathrm{NO_2^-} \to \mathrm{N_2})$ has supplemented the gaseous loss process of nitrogen and is considered to be a major breakthrough in the field of nitrogen cycling in this century, providing

Supported by the Open Fund for Key Laboratory of Land Degradation and Ecological Restoration in Northwestern China of Ningxia University, Project No. LDER2023Q03; by the Open Research Fund of Environmental Protection Key Laboratory of Estuarine and Coastal Environment, Chinese Research Academy of Environmental Sciences, Project No. HKHA2022009, and by the Fundamental Research Funds for the Central Public-Interest Scientific Institution, Project No. 2022YSKY-03.

²College of Application of Engineering, Henan University of Science and Technology, Sanmenxia, P.R. China

³Engineering Technology Research Center of Sanmenxia Yellow River Wetland Environmental Process and Ecological Restoration, Sanmenxia, P.R. China

^{*}Corresponding authors: guanqingsong163@163.com; nxuliu2012@126.com

[©] The authors. This work is licensed under a Creative Commons Attribution-NonCommercial 4.0 International (CC BY-NC 4.0).

new insights for nitrogen cycling research (Mulder et al. 1995, Dalsgaard et al. 2003, Jensen et al. 2008, Canfield et al. 2010). Recent studies have identified another significant nitrogen removal pathway, i.e., ferric iron reduction coupled with anaerobic ammonium oxidation (Feammox). The characteristics of Feammox in tropical rainforest soil (Yang et al. 2012), paddy field soil (Ding et al. 2014, Jiang et al. 2023, Ma et al. 2024), the tidal flat wetland in the Yangtze River Estuary (Li et al. 2015), riparian soil (Ding et al. 2017), and alluvial-lacustrine aquifer system (Xiong et al. 2022), have been reported.

However, 3 nitrogen pathways have not been studied in a specific natural ecosystem, the Yellow River wetland. The Yellow River wetland is a typical saline-alkali ecosystem; the sediment parent is sand, resulting in a low content of organic matter (Guan 2022). Therefore, a scientific question is whether the characteristics of denitrification and Anammox and Feammox in the Yellow River wetland are different from other ecosystems. Low organic matter may reduce the abundance of nitrogen-cycling microorganisms, so we hypothesise that the rates of three nitrogen loss pathways were lower than those in other high organic carbon ecosystems.

In this study, we focused on the Yellow River wetlands in the upper reaches of the Yellow River. Isotope tracing, metagenomic, and fluorescence quantitative polymerase chain reaction (Q-PCR) techniques were used to quantitatively analyse the

denitrification, Anammox, and Feammox rates to determine the nitrogen loss characteristics of the Yellow River wetlands and to identify the functional microorganisms and genes related to nitrogen loss.

MATERIAL AND METHODS

Site description and sediment sampling. The sampling site is located in the upper reaches of the Yellow River, Tianhewan Yellow River National Wetland Park, Yinchuan, Ningxia Province. The mainstream of the Yellow River flows through the Yinchuan Plain for 190 km, with a river span of 2.1-6.1 km and a river width of 0.35–1.45 km. The Yinchuan Plain is a typical alluvial plain and is located in an arid to semi-arid region with sparse precipitation and strong evaporation. The average annual precipitation is 180–200 mm, the average annual evaporation is 1 100-1 600 mm, and the altitude range is 1 100-1 200 m a.s.l. The total area of the Tianhewan Yellow River National Wetland is about 900 km². It should be noted that the Yinchuan Plain is characterised by relatively low human interference and a high development level. The dominant plant community is reeds, with a coverage rate of over 90%. Samples were collected from four sampling sites in May 2023, a reed (Phragmites australis (Cav.) Steud.) covered site (LW), a topsoil tillage after harvesting reed site (GD), an artificial grassland covered site (CD), and a poplar covered site (YD) (Figure 1). We collected three surface soil

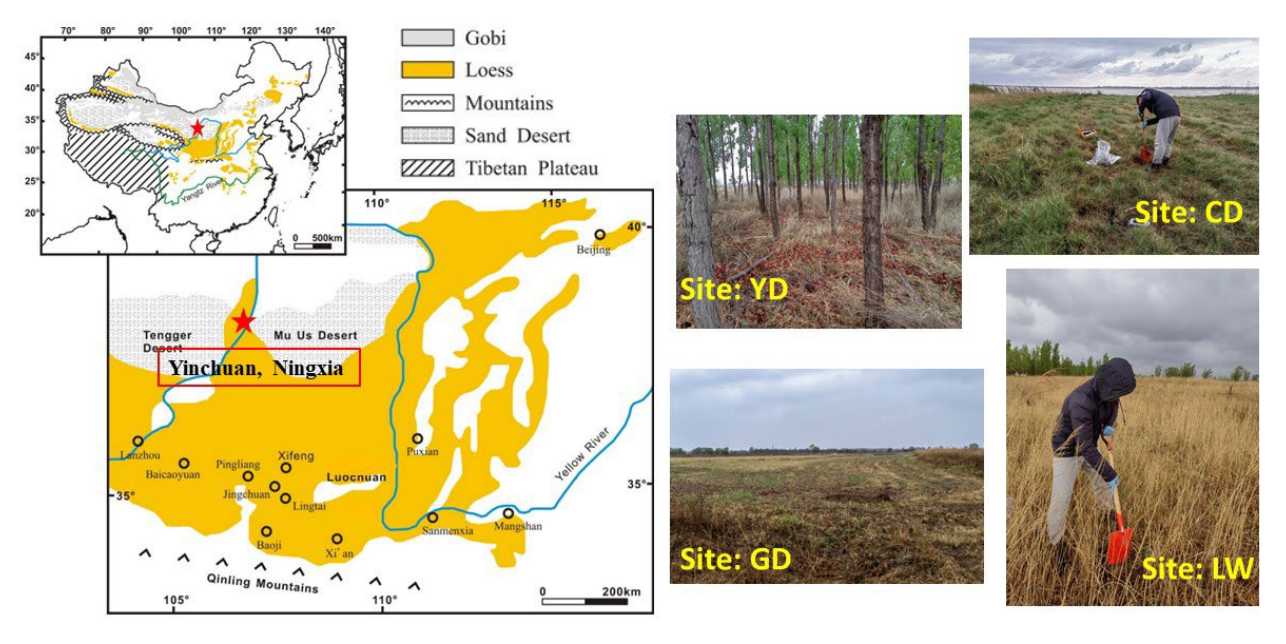


Figure 1. Locations of the sampling sites. YD – poplar covered site; CD – artificial grassland covered site; GD – topsoil tillage after harvesting reed site; LW – covered site

Table 1. Possible processes of $^{29}\mathrm{N}_2$ and $^{30}\mathrm{N}_2$ generation from $^{15}\mathrm{NH}_4^+$ under anaerobic conditions

Product	Nitrogen substrate 1	Nitrogen substrate 2	Process	
	added $^{15}\mathrm{NH_4^+}$	added $^{15}\mathrm{NH_4^+}$	Feammox to N_2	
$^{30}N_{2}$	added $^{15}\mathrm{NH_4^+}$	Feammox-generated $^{15}\mathrm{NO}^2$ and $^{15}\mathrm{NO}^3$	Anammox	
	Feammox-generated $^{15}\mathrm{NO}_2^-$ and $^{15}\mathrm{NO}_3^-$	Feammox-generated $^{15}\mathrm{NO}_2^-$ and $^{15}\mathrm{NO}_3^-$	denitrification	
²⁹ N ₂	added $^{15}\mathrm{NH_4^+}$	background $^{14}\mathrm{NH_4^+}$	Feammox to N_2	
	added $^{15}\mathrm{NH_4^+}$	Feammox-generated $^{14}\mathrm{NO}_2^-$ and $^{14}\mathrm{NO}_3^-$	Anammox	
	Feammox-generated $^{15}\mathrm{NO}^2$ and $^{15}\mathrm{NO}^3$	background $^{14}\mathrm{NH_4^+}$	Anammox	
	Feammox-generated ¹⁵ NO ₂ and ¹⁵ NO ₃	Feammox-generated $^{14}\mathrm{NO}_2^-$ and $^{14}\mathrm{NO}_3^-$	denitrification	

samples (0–10 cm) within a 3 m² area at each site, thoroughly combined the three samples, placed them in a portable refrigerator, and transferred them to the laboratory as quickly as possible for isotope and physicochemical analyses. A 50 mL sterilised centrifuge tube was filled with soil and stored in dry ice before metagenomic and Q-PCR analyses.

Isotopic tracer incubations. The isotope experiments were conducted in an anaerobic glove box filled with helium. First, ultrapure water was purged with helium for 10 min. Then, the sediments were mixed with ultrapure water at a 1:1 mass ratio according to the wet weight of the sediment. The mixture was stirred while being purged with helium for 10 min to produce anaerobic mud. The mud was pre-incubated in an anaerobic glove box for 2 days to remove residual oxygen, nitrate, and nitrite.

The pre-culture mud was transferred into a 120 mL vial and overflowed. The vial was then sealed with a rubber stopper and an aluminium cap. Two sets of conditions were prepared for the Feammox experiments: (1) $^{15}{\rm NH_4Cl}$ (98% $^{15}{\rm N}$, Sigma-Aldrich, St. Louis, USA) and (2) $^{15}{\rm NH_4}$ + Fe $^{\rm (III)}$. Subsequently, 100 µL of $^{15}{\rm NH_4Cl}$ was added using a micro-injector, and the final $^{15}{\rm NH_4Cl}$ concentration was 100 µmol/L. Fe $^{\rm (III)}$ (FeCl $_3$ solution) was added at a 6:1 ratio (Fe $^{\rm (III)}$: $^{15}{\rm NH_4}^+$). The incubation time was set to 0, 3, 6, 9 and 12 days. At each time point, 200 µL of saturated HgCl solution was injected into the vial to terminate the reactions.

For the Anammox and denitrification incubations, the pretreatment was the same as the Feammox experiment. 100 μL of $Na^{15}NO_3$ (98% ^{15}N , Sigma-Aldrich, St. Louis, USA) were extracted and transferred into the vial. The final $^{15}NO_3^-$ concentration was 100 $\mu mol/L$. The incubation time was set to 0, 1, 3, 5 and 7 days. Also, 200 μL of saturated HgCl solution was injected into the vial to terminate the reactions.

The $^{29}\mathrm{N}_2$ and $^{30}\mathrm{N}_2$ in the slurries were measured using a GasBench II-Delta V Advantage isotope ratio mass spectrometer (Thermo Fisher, Bremen, Germany). The rates of production of $^{29}\mathrm{N}_2$ and $^{30}\mathrm{N}_2$ were calculated based on the slope of the fitted linear. $^{29}\mathrm{N}_2$ and $^{30}\mathrm{N}_2$ were produced through three pathways, i.e., Feammox, Anammox, and denitrification (Table 1). Therefore, to conservatively estimate the Feammox rate, the potential Feammox rate is reported for the production of $^{30}\mathrm{N}_2$. The calculation details of denitrification and Anammox rates have been reported in previous studies (Thamdrup and Dalsgaard 2002, Guan et al. 2019).

Metagenomic sequencing. The metagenomic sequencing analysis was conducted by the Shanghai Mei Ji Biomedical Technology Co., Ltd. The functional genes for denitrification (narG: nitrate reductase gene; nirS/nirK: nitrite reductase genes; norB: nitric oxide reductase gene; and nosZ: nitrous oxide reductase gene), Anammox (hzsA: N_2H_4 synthase gene; and hzo: N_2H_4 oxidoreductase), dissimilatory nitrate reduction to ammonium (DNRA) (napA: nitrate

Table 2. Characteristics of water

Site	Temperature	Conductivity (µS/cm)	11	Eh	DO	NO_3^N	NO_2^N	NH ₄ +N	T Fe	Fe ^(II)	Fe ^(III)			
	(°C)	$(\mu S/cm)$	рп	(mV)	ЪО			(mg	g/L)					
Yinchuan	13	810	8.46	275.6	5.97	1.825 ± 0.015	0.022 ± 0.000	0.277 ± 0.006	0.357 ± 0.012	0.135 ± 0.004	0.222			

Eh - oxidation-reduction potential; DO - dissolved oxygen; T Fe - total hydrochloric acid-extractable iron

Table 3. Chemical characteristics of sediments

Site Ter	Temperature	ъЦ	Eh (mV)		TON	NO ₃ -N	NO ₂ -N	NH ₄ ⁺ -N	T Fe	Fe ^(II)	Fe ^(III)	Moisture
	Temperature (°C)	рп		(9	(%)		(mg/kg)					content (%)
LW	11.6	7.97	396	0.37	0.04	4.3 ± 0.6^{a}	0.00	$42 \pm 2^{\rm b}$	203 ± 2^{a}	34 ± 1^a	170 ± 3 ^a	18.21
CD	13.1	7.96	355	0.55	0.06	5.5 ± 0.3^{a}	0.02	$40\pm2^{\rm b}$	$420\pm6^{\rm d}$	$56 \pm 0^{\rm b}$	$364 \pm 6^{\rm d}$	22.43
YD	10.1	7.79	375	0.41	0.04	6.4 ± 0.5^{b}	0.02	77 ± 2^{c}	385 ± 9^{c}	$59 \pm 0^{\mathrm{b}}$	326 ± 9 ^c	24.25
GD	11.8	8.7		0.40	0.04	$21.3 \pm 0.1^{\rm c}$	0.28	21 ± 1^a	355 ± 5^{b}	80 ± 1^{c}	$275 \pm 5^{\rm b}$	19.34

n = 3, the same letter indicates no significant difference at P < 0.05. LW – covered site; CD – artificial grassland covered site; YD – poplar covered site; GD – topsoil tillage after harvesting reed site; Eh – oxidation-reduction potential; TOC – total organic carbon; TON – total organic nitrogen; T Fe – total hydrochloric acid-extractable iron

dissimilatory reductase gene; *nrfA*), and Feammox (*Acidimfcrobiaceae A6*) were analysed *via* fluorescence Q-PCR.

Sample analysis. The pH, temperature, and other water parameters were measured using a portable water quality parameter analyser (DZB-712F, Shanghai, China). The sediment-water contents were determined

from the weight lost from a known amount of wet sediments that had been dried at 60 °C to a constant value. The pH of sediment was measured with deionised water at a ratio of 1:2.5 (10 g:25 mL). The total organic carbon (TOC) and total organic nitrogen (TON) contents were determined using an elemental analyser (Thermo Fisher Flash 2000 CHNS/O, Waltham, USA).

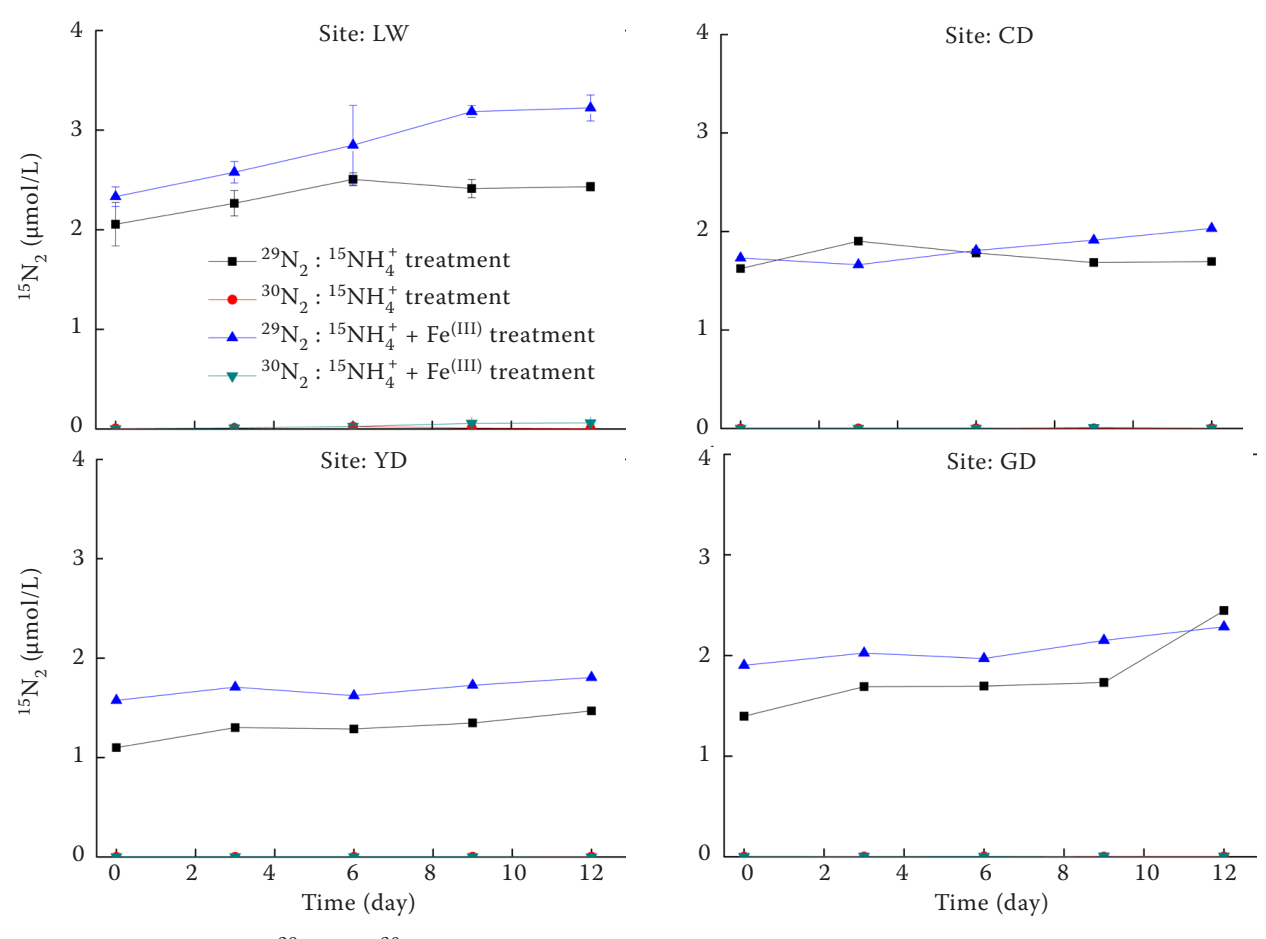


Figure 2. Production of $^{29}N_2$ and $^{30}N_2$ in incubations *via* Feammox for the four samples. The error bars represent the standard deviations of three replications. LW – covered site; CD – artificial grassland covered site; YD – poplar covered site; GD – topsoil tillage after harvesting reed site

In the sediments, the KCl-extractable $\mathrm{NH_4^+}$, $\mathrm{NO_3^-}$, and $\mathrm{NO_2^-}$ were extracted with a 2 mol/L KCl solution and determined with a continuous-flow nutrient autoanalyser. The hydrochloric acid-extractable total iron and hydrochloric acid-extractable Fe^(II) were measured using ferrozine staining and UV spectrophotometry (Lovley and Phillips 1987).

Statistical analysis. One-way analysis of variance (ANOVA) was conducted to analyse the different physical-chemical properties and the differences in the 30 N $_2$ and 29 N $_2$ production rates. The significance was $\alpha = 0.05$. The statistical analysis was conducted using the SPSS 25.0 software (SPSS Inc., Chicago, USA), and the figures were plotted using Origin Pro 8 (Northampton, USA).

RESULTS

Chemical characteristics of the sediments. The pH of the water was alkaline, and the oxidation-

reduction potential (Eh) value indicated that the water was in an oxidised state. The $Fe^{(III)}$ content, which accounted for 63%, was higher than the $Fe^{(III)}$ content. The main form of inorganic nitrogen was nitrate, accounting for 86% (Table 2). The pH of the sediment was alkaline, ranging from 7.79 to 8.7. The main form of inorganic nitrogen was ammonium, accounting for 90% (LW), 88% (CD), 92% (YD), and 50% (GD) of the inorganic nitrogen in the four sample sites. The proportions of $Fe^{(III)}$ in the total iron were 84% (LW), 86% (CD), 85% (YD), and 77% (GD). The TOC content ranged from 0.37% to 0.55%, the TON content ranged from 0.04% to 0.06%, and the moisture content ranged from 18.21% to 24.25% (Table 3).

Incubation of Feammox. In the Feammox incubation experiments, the accumulation of $^{29}\mathrm{N}_2$ was detected, and it increased over time. Adding Fe^(III) increased the concentration of the accumulated $^{29}\mathrm{N}_2$, but no $^{30}\mathrm{N}_2$ accumulation was detected. The gas accumulation rate was the fastest in the sample from

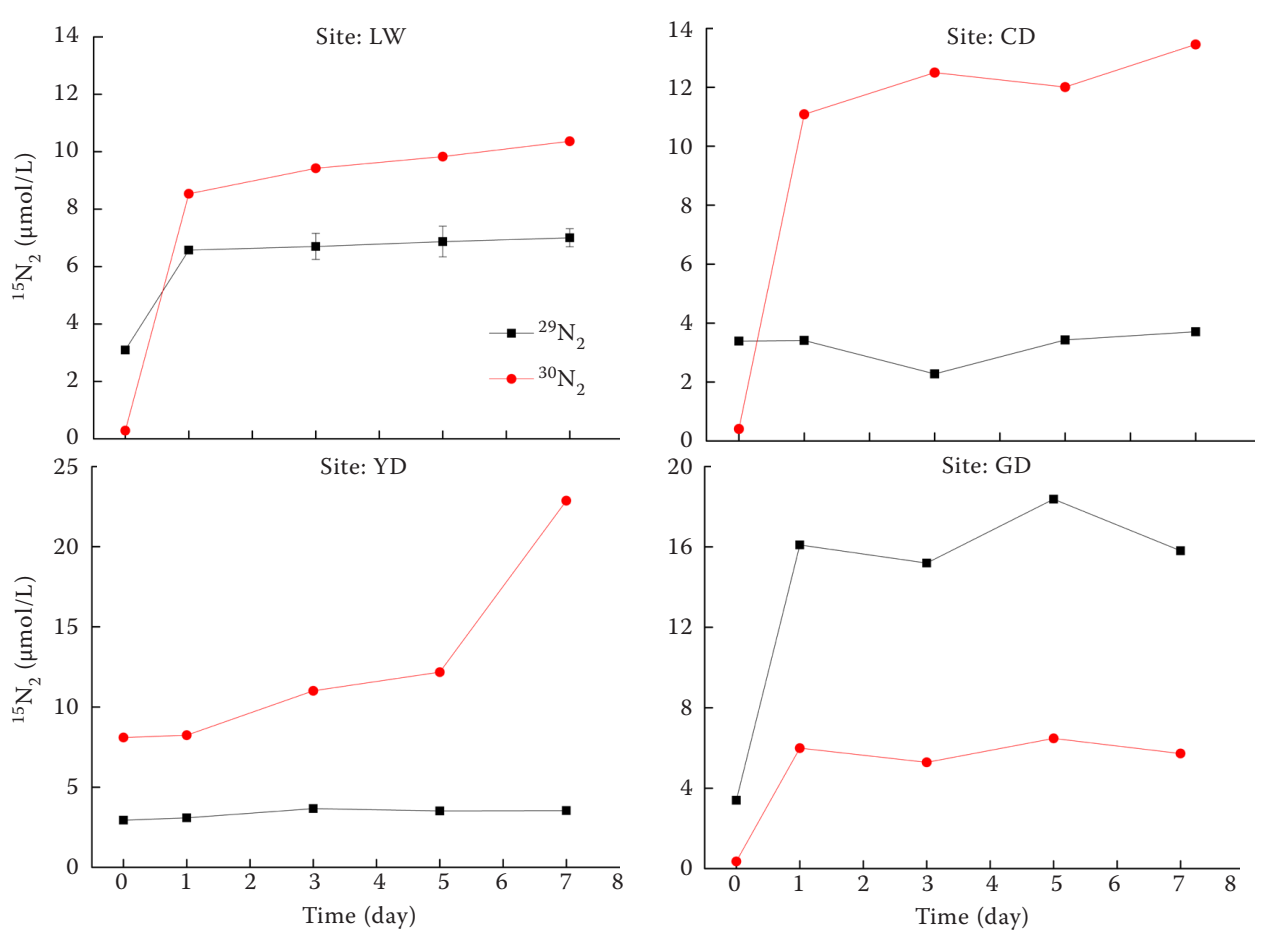


Figure 3. Production of $^{29}\mathrm{N}_2$ and $^{30}\mathrm{N}_2$ incubations via denitrification and Anammox. The error bars represent the standard deviations of three replications. LW – covered site; CD – artificial grassland covered site; YD – poplar covered site; GD – topsoil tillage after harvesting reed site

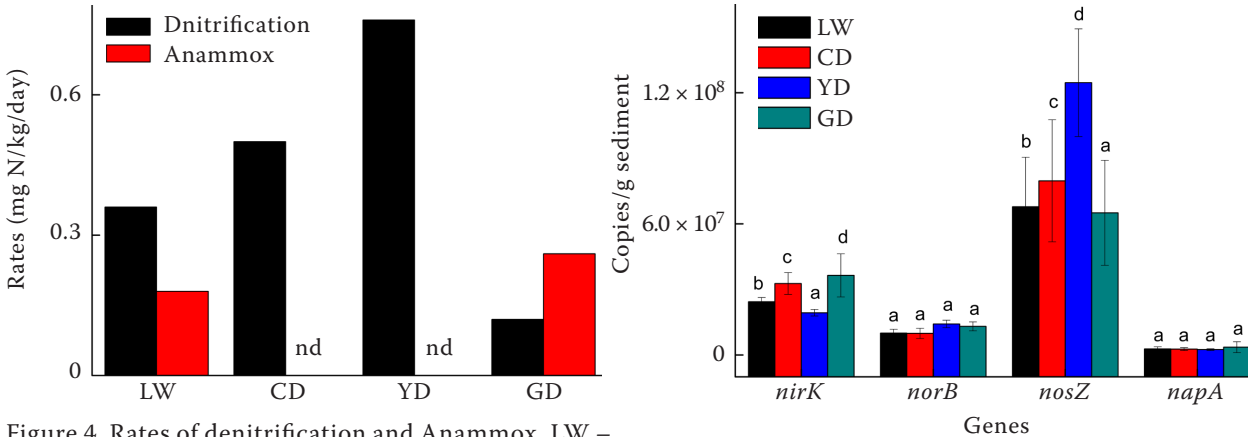


Figure 4. Rates of denitrification and Anammox. LW – covered site; CD – artificial grassland covered site; YD – poplar covered site; GD – topsoil tillage after harvesting reed site; nd – not detected

the LW site and reached the maximum value after 12 days. The gas accumulation concentration of the sample from the CD site was the lowest (Figure 2). The results indicate no $^{30}{\rm N}_2$ accumulation was detected, and the Feammox process was weak.

Incubation of denitrification and Anammox. Both $^{29}\mathrm{N}_2$ and $^{30}\mathrm{N}_2$ were detected in the samples from the LW and GD sites, and the concentration increased with the increase of incubation time. Only $^{30}\mathrm{N}_2$ was detected in the samples from the CD and YD sites. The concentration of $^{30}\mathrm{N}_2$ was higher than the $^{29}\mathrm{N}_2$ concentration except for site GD (Figure 3). The max concentrations of $^{29}\mathrm{N}_2$ and $^{30}\mathrm{N}_2$ were 15.80 (GD) and 22.86 (YD) µmol/L. Figure 4 shows that the denitrification rates were 0.36 (LW), 0.5

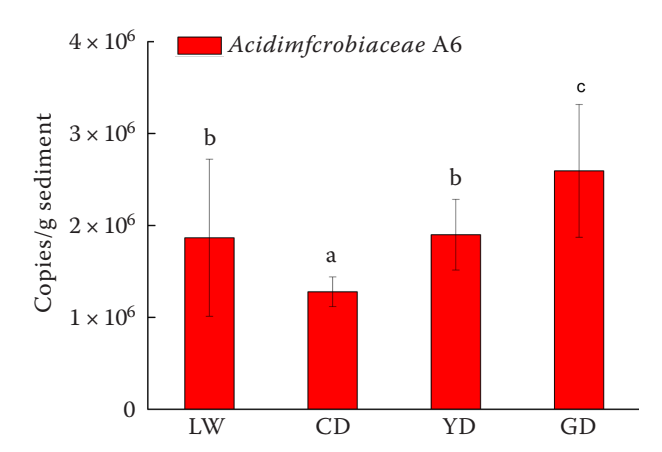


Figure 6. Abundance of *Acidimfcrobiaceae* A6. The error bars represent the standard deviations of three replications. LW – covered site; CD – artificial grassland covered site; YD – poplar covered site; GD – topsoil tillage after harvesting reed site

Figure 5. Abundances of functional genes. The error bars represent the standard deviations of three replications. LW – covered site; CD – artificial grassland covered site; YD – poplar covered site; GD – topsoil tillage after harvesting reed site

(CD), 0.76 (YD) and 0.12 (GD) mg N/kg/day, and the Anammox rates were 0.18 (LW) and 0.26 (GD) mg N/kg/day, CD and YD sites did not detect Anammox.

Abundances of functional genes. Four functional genes were detected, including three denitrification genes (nirK, norB, nosZ, and napA) and one DNRA gene (napA). However, the Anammox functional gene was not detected. The gene abundance order was as follows: nosZ > nirK > norB > napA (Figure 5). The content of *nirK* is range from $1.93 \times 10^7 \pm 1.5 \times$ $10^6 \text{ to } 3.64 \times 10^7 \pm 9.88 \times 10^6 \text{ copies/g sediment; the}$ content of *norB* is range from $9.88 \times 10^6 \pm 2.34 \times 10^8 \pm 10^$ 10^6 to $1.42 \times 10^7 \pm 1.70 \times 10^6$ copies/g sediment; the content of *nosZ* is range from $1.24 \times 10^8 \pm 2.46 \times 10^8 \pm 1.008 \pm 1.000$ $10^7 \text{ to } 6.50 \times 10^7 \pm 2.40 \times 10^7 \text{ copies/g sediment; the}$ content of *napA* is range from $2.45 \times 10^6 \pm 3.59 \times 10^8 \times 10^$ 10^5 to $3.57 \times 10^6 \pm 2.48 \times 10^6$ copies/g sediment. The sample from the YD site had the greatest abundance of denitrification genes. The order of the abundances of the Feammox functional bacteria was as follows: GD > YD > LW > CD (Figure 6), and the content of Acidimfcrobiaceae A6 are $2.59 \times 10^6 \pm 7.23 \times 10^5$, $1.89 \times 10^6 \pm 3.84 \times 10^5$, $1.86 \times 10^6 \pm 8.54 \times 10^5$ and $1.27 \times 10^6 \pm 1.62 \times 10^5$ copies/g sediment.

DISCUSSION

The contribution of Feammox to nitrogen loss was low. The Feammox rate of the Yellow River wetland was lower than that of other types of wetlands (Table 4). The organic carbon, dissolved oxygen, and iron oxide morphology have also been demonstrated

Table 4. Rates of Feammox and ecosystem nitrogen loss in different types of soil

Types	Feammox rates (mg N/kg/day)	Nitrogen loss th (t N/kr	Reference	
Yellow river wetlands	none			this study
Tropical forest soils	0.32	0.1 - 0.4	(0-10 cm)	Yang et al. (2012)
Paddy soils	0.17 - 0.59	0.78 - 6.1	(0-10 cm)	Ding et al. (2014)
Yangtze estuary	0.24-0.36	11.5-18	(0-5 cm)	Li et al. (2015)
Riparian zone	0.32 - 0.37	2.4-4.4	(0-10 cm)	Ding et al. (2017)
Mangroves	0.38 - 0.48	6.26	(0-5 cm)	Guan et al. (2018)
Paddy soils	0.42-65.68			Li et al. (2019)

to affect Feammox activity significantly (Huang et al. 2016). The most typical characteristics of the Yellow River wetlands are a low organic carbon content and very low nutrient content (Li et al. 2022, Guan and Li 2023), which result in a low microbial abundance and slow biogeochemical cycling of elements. The Yellow River wetland is generally not flooded and has a high Eh value, and as a result, the reduction of $Fe^{(III)}$ is weak. The pH is the environmental factor that has the greatest impact on Feammox microorganisms. From a thermodynamic perspective, under the condition of pH > 6.5, the Gibbs free energy of the reaction is greater than zero, so the reaction cannot occur spontaneously. The above reasons lead to the weak Femmox in the Yellow River wetland.

However, research has shown that Feammox can still be detected in alkaline soils. This is most likely due to the microbial function of Feammox. Using molecular biology techniques, scholars have discovered a close relationship between iron-reducing bacteria and the Feammox reaction, among which *Geobacter* and *Anaeromyxobacter* are the main microorganisms driving the Feammox process (Zhou et al. 2016). Li et al. (2019) analysed the functional microorganisms involved in the Feammox process in paddy soil using ribonucleic acid-stable isotope probe technology (RNA-SIP) and found that *Geobacter*, *GOUTA19*, *Nitrosophaeraceae*, and *Pseudomonas* were the main microorganisms that potentially drove the Femmox process in this soil (Li et al. 2019).

At present, only one strain with Feammox activity has been isolated. Through 16S ribosomal RNA (rRNA) gene sequencing, it has been determined that this strain belongs to *Acidomycetes*, and thus, it has been named *Acidomycobiaceae* sp. A6 (Huang et al. 2018). The abundance of *Acidimiprobiaceae* sp. A6 is only one-tenth that in rice fields (Yi et al. 2019). Some results show that a major hydrologic

storm event can result in an increase in Fe^(III) and an increase in the abundance of Fe-reducing bacteria, including *Acidimicrobium* sp. A6 (Sherman et al. 2023). The low abundances of functional microorganisms involved in Feammox resulted in Feammox being weak in the Yinchuan Yellow River wetland.

Denitrification is the dominant pathway of nitrogen loss. The denitrification and Anammox rates indicate that denitrification was the main pathway for nitrogen loss in the Yellow River wetland, except for in the GD site. Anammox was also an important nitrogen loss pathway in the LW and GD sites. The Anammox rate was higher than the denitrification rate in the GD site, indicating that topsoil turnover promotes the Anammox process. The YD site had the highest abundance of denitrification genes, which was consistent with the denitrification rate. The total nitrogen loss rates were 0.54 (LW), 0.5 (CD), 0.76 (YD), and 0.38 (GD) mg N/kg/day. The abundance of denitrification functional genes was consistent with the denitrification rate, and denitrification and Anammox were the main nitrogen loss pathways. The dominant nitrogen loss pathways varied in the sites with different vegetation cover types. Anammox was the dominant nitrogen loss pathway in the artificial grassland-covered site, and denitrification was the dominant pathway in the other sites.

Acknowledgement. We are thanks to Third Institute of Oceanography providing nitrogen isotope analysis.

REFERENCES

Canfield D.E., Glazer A.N., Falkowski P.G. (2010): The evolution and future of earth's nitrogen cycle. Science, 330: 192–196.

Dalsgaard T., Canfield D.E., Petersen J., Thamdrup B., Acuña-González J. (2003): N₂ production by the anammox reaction in

- the anoxic water column of golfo dulce, costa rica. Nature, 422: 606-608
- Delwiche C.C., Bryan B.A. (1976): Denitrification. Annual Review of Microbiology, 30: 241–262.
- Ding B., Li Z., Qin Y. (2017): Nitrogen loss from anaerobic ammonium oxidation coupled to iron⁽ⁱⁱⁱ⁾ reduction in a riparian zone. Environmental Pollution, 231: 379–386.
- Ding L.J., An X.L., Li S., Zhang G.L., Zhu Y.G. (2014): Nitrogen loss through anaerobic ammonium oxidation coupled to iron reduction from paddy soils in a chronosequence. Environmental Science and Technology, 48: 10641–10647.
- Fowler D., Pyle J.A., Raven J.A., Sutton M.A. (2013): The global nitrogen cycle in the twenty-first century: introduction. Philosophical Transactions of the Royal Society B-Biological Sciences, 368: 0164.
- Gruber N., Galloway J.N. (2008): An earth-system perspective of the global nitrogen cycle. Nature, 451: 293–296.
- Guan Q., Zhang Y., Tao Y., Chang C.-T., Cao W. (2019): Graphene functions as a conductive bridge to promote anaerobic ammonium oxidation coupled with iron reduction in mangrove sediment slurries. Geoderma, 352: 181–184.
- Guan Q. (2022): Vertical distribution characteristics and source tracing of organic carbon in sediment of the yellow river wetland, Sanmenxia, China. Limnologica, 93: 125960.
- Guan Q., Li Q. (2023): Denitrification prevails over anammox in the yellow river wetland, Sanmenxia, China. Journal of Soils and Sediments, 24: 1790–1799.
- Guan Q.S., Cao W.Z., Wang M., Wu G.J., Wang F.F., Jiang C., Tao Y.R., Gao Y. (2018): Nitrogen loss through anaerobic ammonium oxidation coupled with iron reduction in a mangrove wetland. European Journal of Soil Science, 69: 732–741.
- Huang S., Chen C., Peng X., Jaffé P.R. (2016): Environmental factors affecting the presence of acidimicrobiaceae and ammonium removal under iron-reducing conditions in soil environments. Soil Biology and Biochemistry, 98: 148–158.
- Huang S., Jaffé P., Senko J.M. (2018): Isolation and characterization of an ammonium-oxidizing iron reducer: *Acidimicrobiaceae* sp. A6. Plos One, 13: 0194007.
- Jensen M.M., Kuypers M.M.M., Lavik G., Thamdrup B. (2008): Rates and regulation of anaerobic ammonium oxidation and denitrification in the black sea. Limnology and Oceanography, 53: 23–36.
- Jiang Y., Liu D., Zhang S., Wei R., Ding X. (2023): Volatile fatty acids changed the microbial community during feammox in coastal saline-alkaline paddy soil. Environmental Science and Pollution Research, 30: 41755–41765.

- Li H., Su J.Q., Yang X.R., Zhou G.W., Lassen S.B., Zhu Y.G. (2019): RNA stable isotope probing of potential feammox population in paddy soil. Environmental Science and Technology, 53: 4841–4849.
- Li T., Zhou Y., Yang F., Guan Q., Li Q., Liang H., Zhao J. (2022): Impact of environmental factors on the diversity of nitrogen-removal bacteria in wetlands in the sanmenxia reservoir of the yellow river. Journal of Soils and Sediments, 23: 512–525.
- Li X.F., Hou L.J., Liu M., Zheng Y.L., Yin G.Y., Lin X.B., Cheng L., Li Y., Hu X.T. (2015): Evidence of nitrogen loss from anaerobic ammonium oxidation coupled with ferric iron reduction in an intertidal wetland. Environmental Science and Technology, 49: 11560–11568.
- Lovley D.R., Phillips E.J.P. (1987): Rapid assay for microbially reducible ferric iron in aquatic sediments. Applied and Environmental Microbiology, 53: 1536–1540.
- Ma D., Wang J., Fang J., Jiang Y., Yue Z. (2024): Asynchronous characteristics of feammox and iron reduction from paddy soils in southern China. Environmental Research, 252: 118843.
- Mulder A., Graaf A.A.V.D., Robertson L.A., Kuenen J.G. (1995): Anaerobic ammonium oxidation discovered in a denitrifying fluidized bed reactor. FEMS Microbiology Ecology, 16: 177–184.
- Niu X., Zhou S., Deng Y. (2021): Advances in denitrification microorganisms and processes. Chinese Journal of Biotechnology, 37: 3505–3519.
- Sherman A.E., Huang S., Jaffé P.R. (2023): Impacts of storm disturbance and the role of the feammox process in high nutrient riparian sediments. Biogeochemistry, 165: 113–128.
- Thamdrup B., Dalsgaard T. (2002): Production of $\rm N_2$ through anaerobic ammonium oxidation coupled to nitrate reduction in marine sediments. Applied and Environmental Microbiology, 68: 1312–1318.
- Xiong Y., Du Y., Deng Y., Ma T., Wang Y. (2022): Feammox in alluvial-lacustrine aquifer system: nitrogen/iron isotopic and biogeochemical evidences. Water Research, 222: 118867.
- Yang W.H., Weber K.A., Silver W.L. (2012): Nitrogen loss from soil through anaerobic ammonium oxidation coupled to iron reduction. Nature Geoscience, 5: 538–541.
- Yi B., Wang H., Zhang Q., Jin H., Abbas T., Li Y., Liu Y., Di H. (2019): Alteration of gaseous nitrogen losses *via* anaerobic ammonium oxidation coupled with ferric reduction from paddy soils in southern China. Science of the Total Environment, 652: 1139–1147.
- Zhou G.W., Yang X.R., Li H., Marshall C.W., Zheng B.X., Yan Y., Su J.Q., Zhu Y.G. (2016): Electron shuttles enhance anaerobic ammonium oxidation coupled to iron(iii) reduction. Environmental Science and Technology, 50: 9298–9307.

Received: June 11, 2024 Accepted: September 19, 2024 Published online: October 9, 2024